Simultaneous photoproduction of neutral and charged pions on the deuteron at ELPH

Takatsugu Ishikawa

Research Center for Electron Photon Science (ELPH), Tohoku University

Contents:

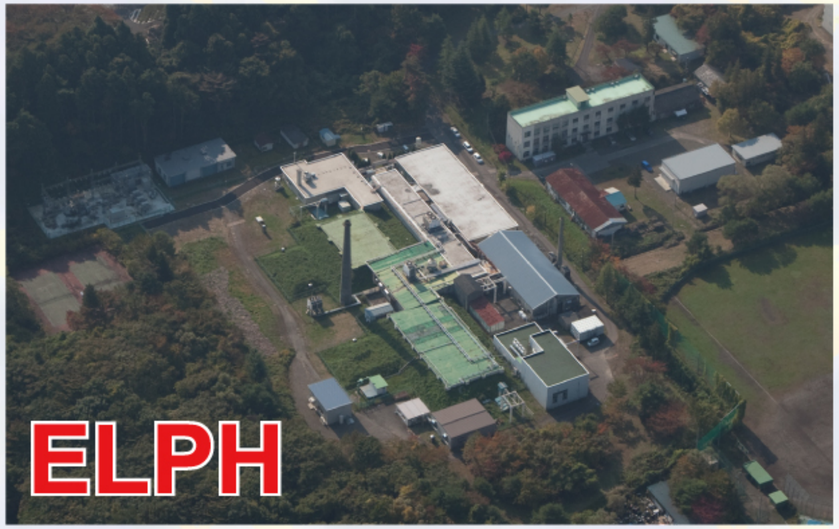

university-based accelerator facility
1.3 GeV bremsstrahlung photon beam

Meson photoproduction for baryon spectroscopy

Baryon spectroscopy:

testing ground for understanding low energy QCD

to figure out new effective degree of freedom

describing hadrons:

diquark correlation, meson-molecule, hybrid, *etc*

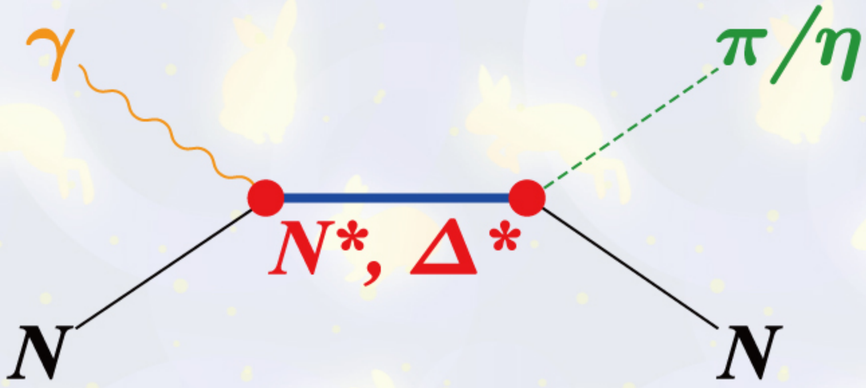

Meson photoproduction

single meson production

$\gamma p \rightarrow \pi^+ n$, $\gamma p \rightarrow \pi^0 p$, $\gamma p \rightarrow \eta p$

multi meson production: hilghly excited baryons

$\gamma p \rightarrow \pi^+ \pi^- p$, $\gamma p \rightarrow \pi^0 \pi^0 p$, $\gamma p \rightarrow \pi^0 \eta p$

$\gamma p \rightarrow \pi^+ \pi^0 n$

Meson photoproduction for baryon spectroscopy

$\gamma p \rightarrow \pi^+\pi^0 n$ reaction

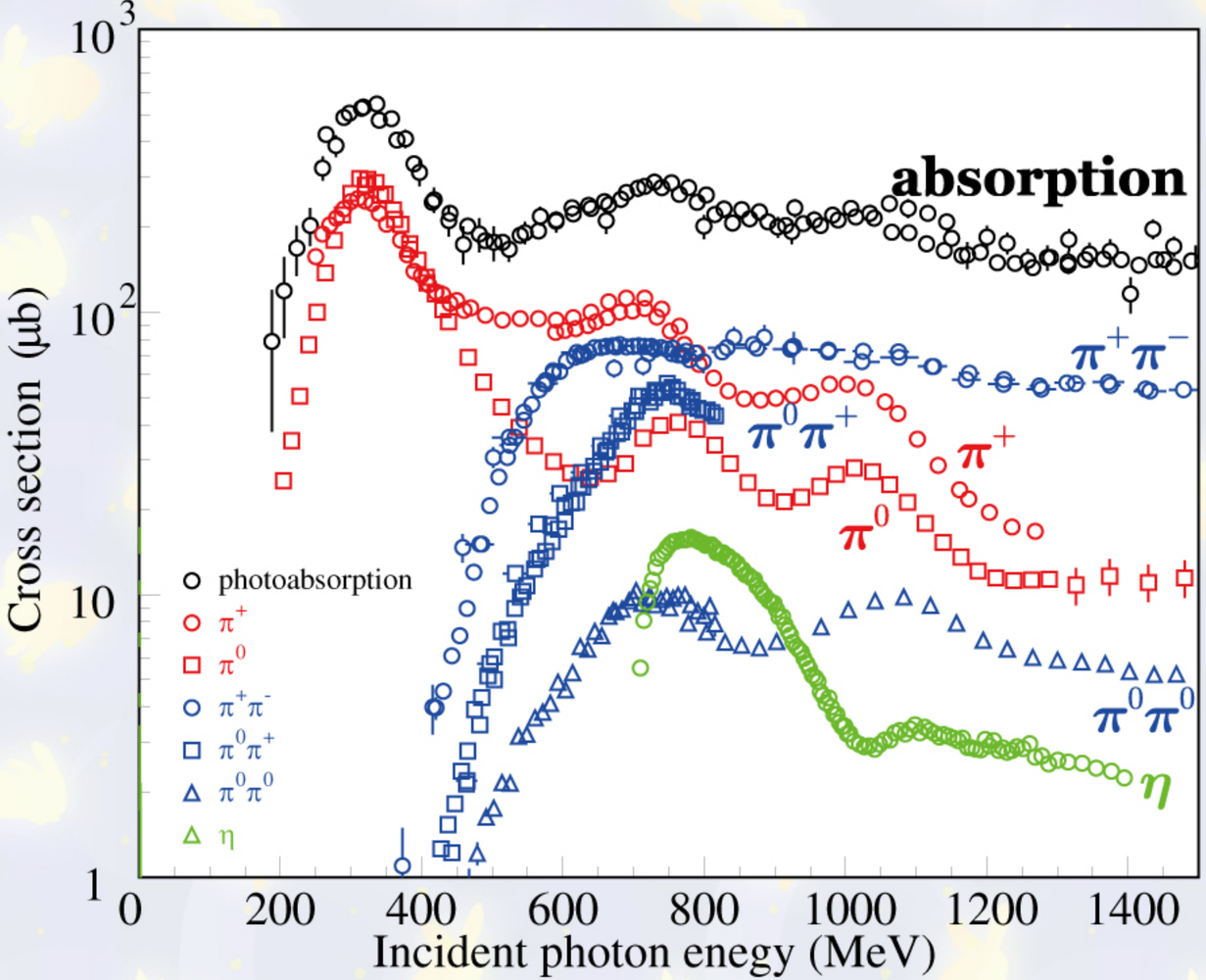

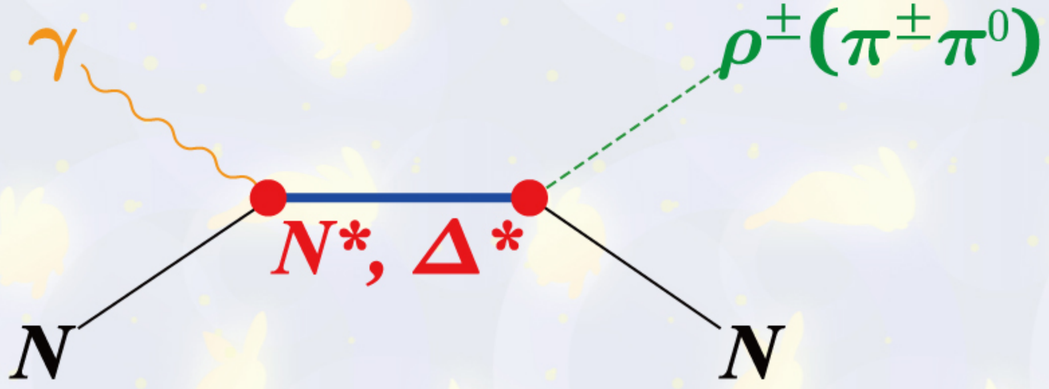

no published data above 800 MeV
baryons coupling to ρN

The neutron target channels are also important for systematic study.

Experimental setup ~ accelerator

Electron Beam **after the earthquake**

LINAC 150 MeV→93 MeV

Booster Ring 1200 MeV (max)

→1300 MeV

Photon Beam

Bremsstrahlung & tagged

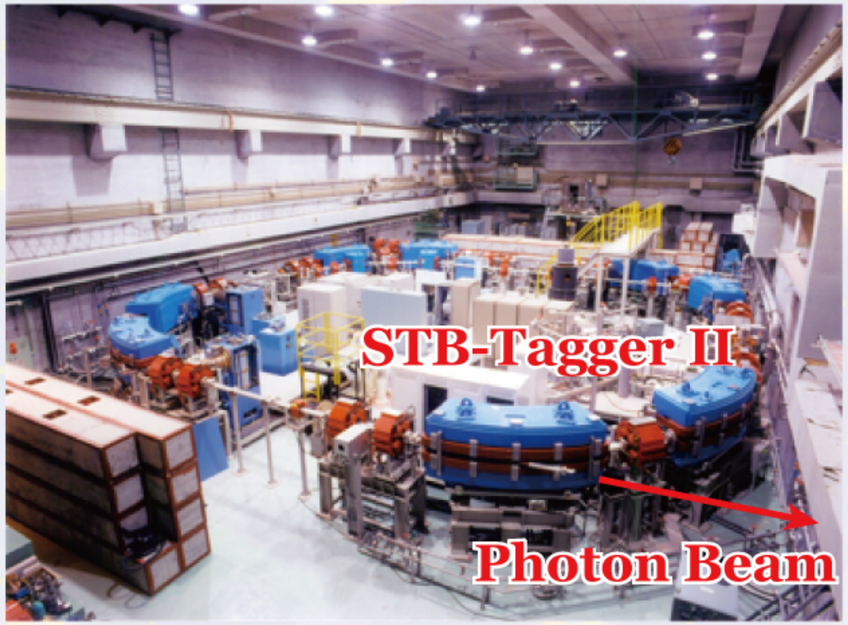

1.3 GeV Booster STorage Ring

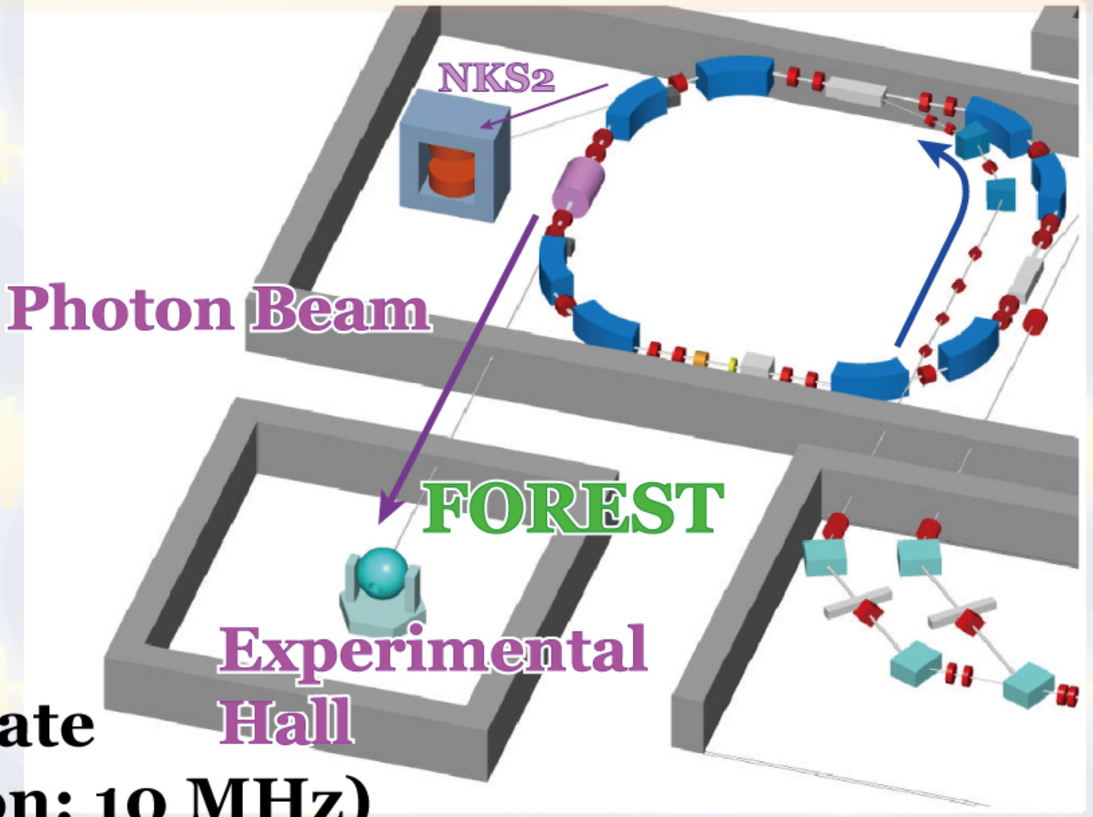

Typical tagging rate

20 MHz (photon: 10 MHz)

Photon beam energy

740~1150 MeV @ 1200 MeV δE: 1~2 MeV

570~890 MeV @ 930 MeV

T. Ishikawa et al., Nucl. Instr. Meth. A 622, 1 (2010);

T. Ishikawa et al., Nucl. Instr. Meth. A 811, 124 (2016).

Experimental setup ~ EM calorimeter

Backward Gamma

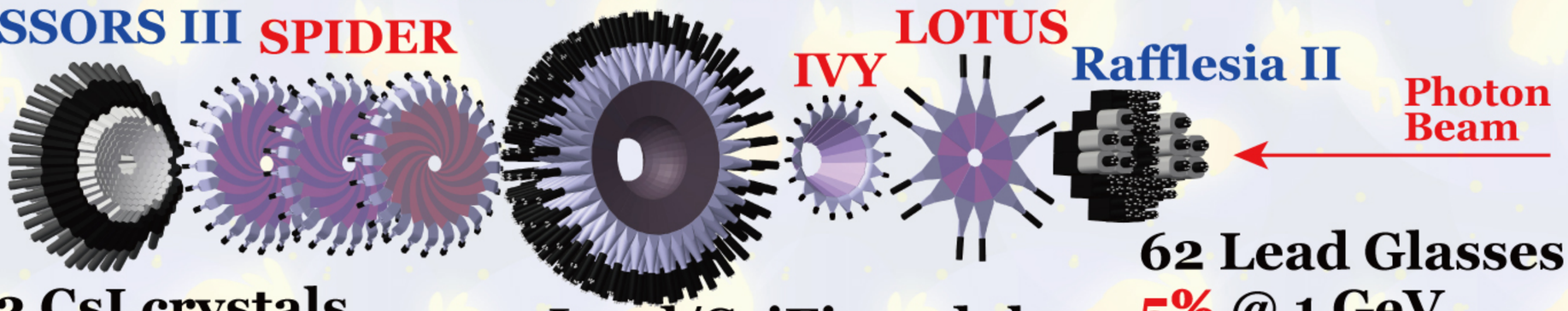

192 CsI crystals
3% @ 1 GeV

252 Lead/SciFi modules
7% @ 1 GeV

62 Lead Glasses
5% @ 1 GeV

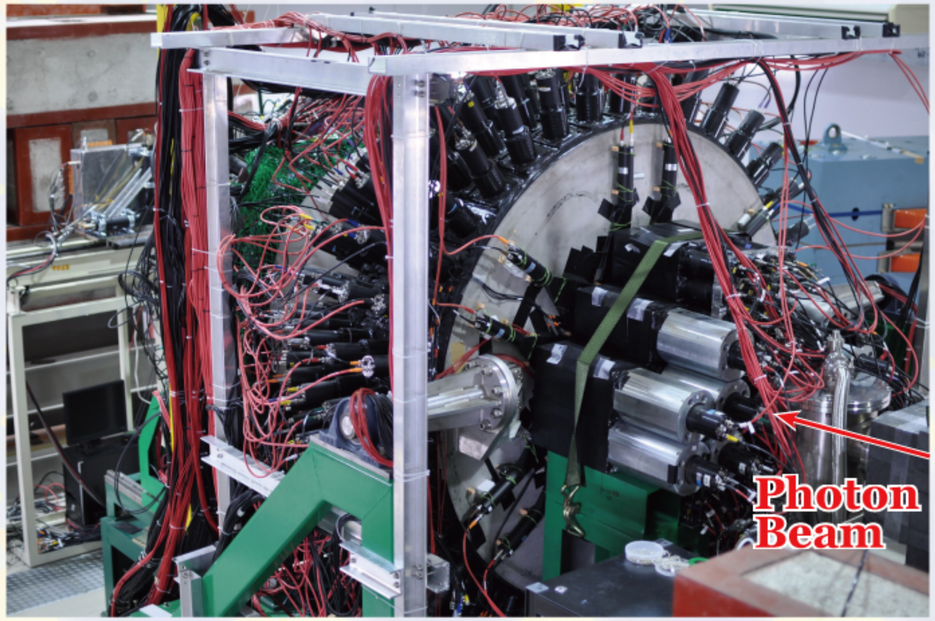

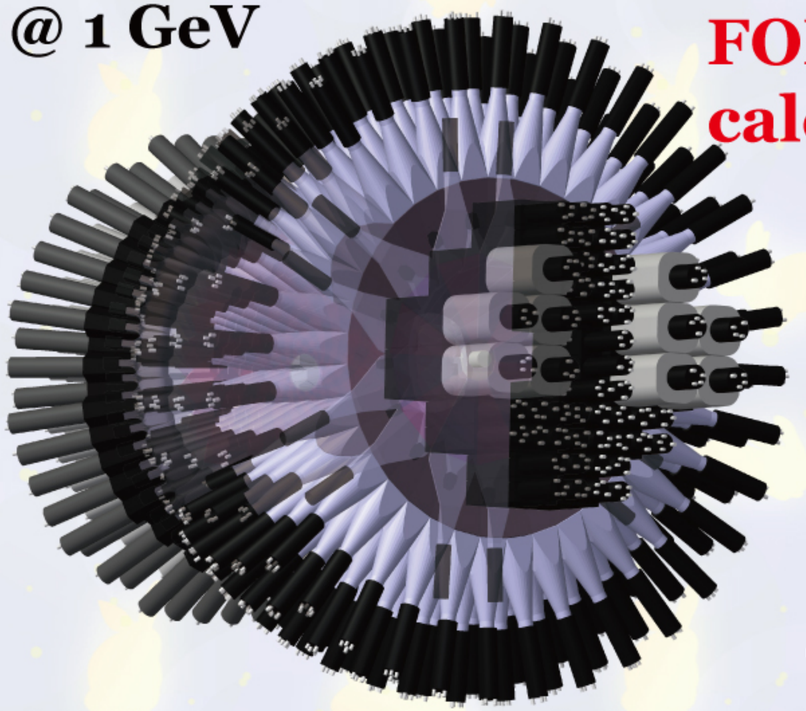

FOREST electro-magnetic calorimeter

Target: 45 mm thick LH2 & LD2

T. Ishikawa et al., Nucl. Instr. Meth. A 832, 108 (2016).

Analysis for the $\gamma p \rightarrow \pi^0 \pi^+ n$ reaction (H_2)

Event selection

$\pi^0 \rightarrow \gamma\gamma$ identification

two neutral clusters

time difference: $-3\sigma_t \sim +3\sigma_t$

$M_{\gamma\gamma}$: 50~220 MeV

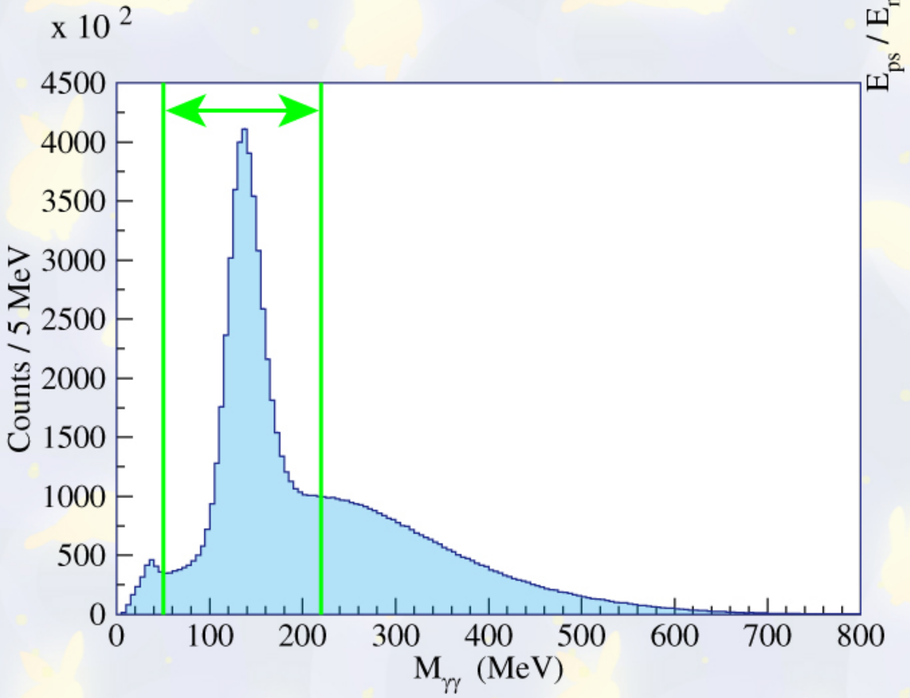

$\pi^{\pm}/p$ identification

using ΔE-E correlation

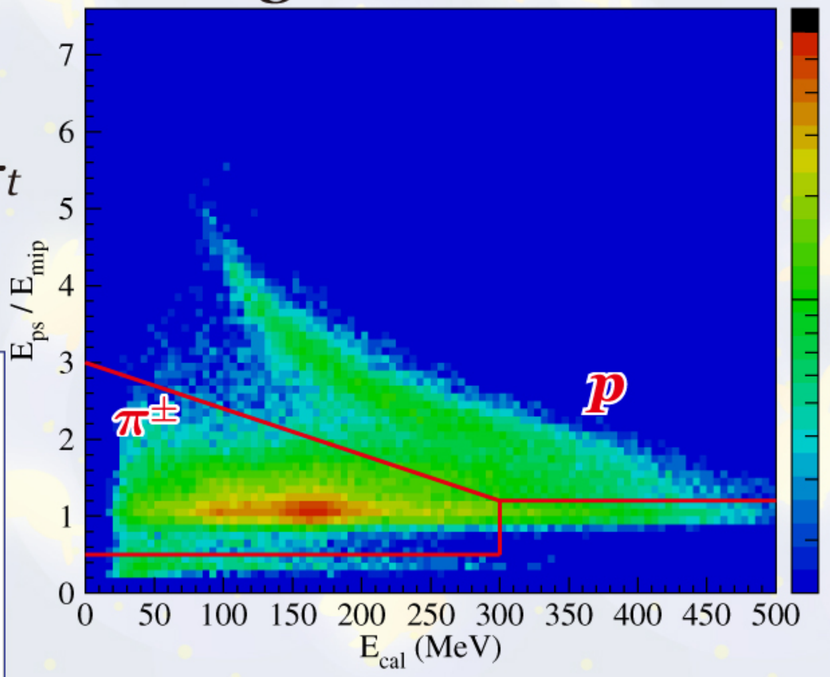

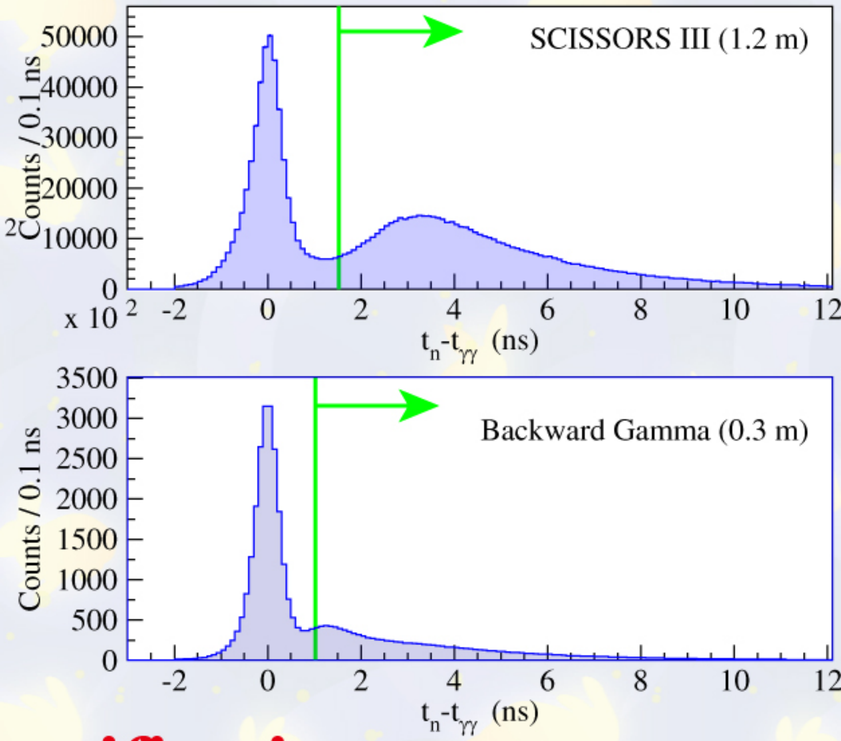

neutron identification

delayed neutral cluster

> 1.5 ns for SCISSORS III

> 1.0 ns for Backward Gamma

Analysis for the $\gamma p \rightarrow \pi^0 \pi^+ n$ reaction (H_2)

Kinematical fit (4C)

constraints

- energy and momentum conservation (4)
- $\gamma\gamma$ invariant mass: π^0 (1)

variables

- incident photon energy (1)
- three-momenta for two γs (2×3)
- three-momentum of the nucleon (3)
- emission angle of the charged pion (2)

the absolute value of the momentum for the charged pion is treated as unmeasured

events in which χ^2 probability≧0.1 are selected

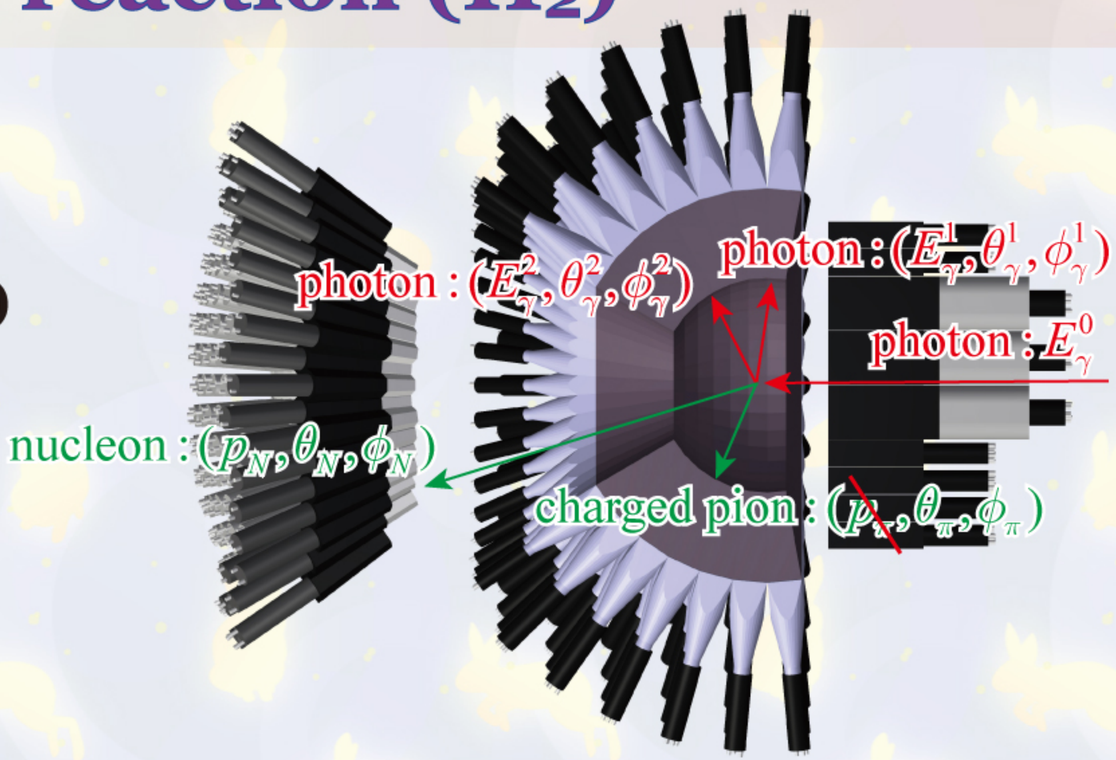

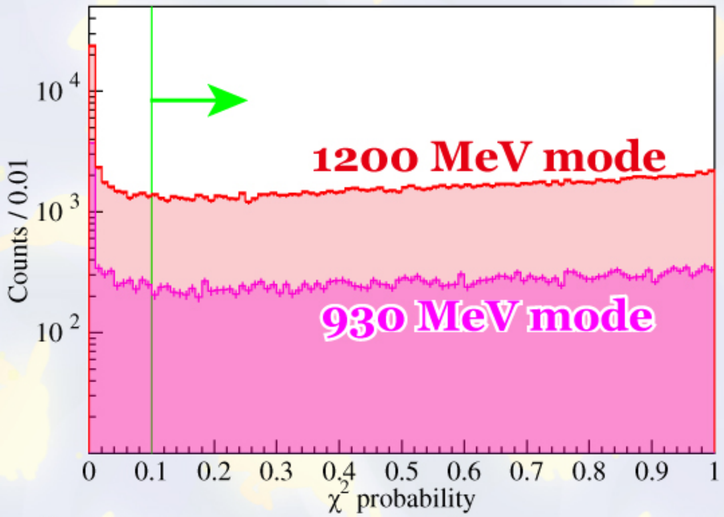

Analysis for the $\gamma p \rightarrow \pi^0\pi^+ n$ reaction (H_2)

Total cross section as a function of E_γ

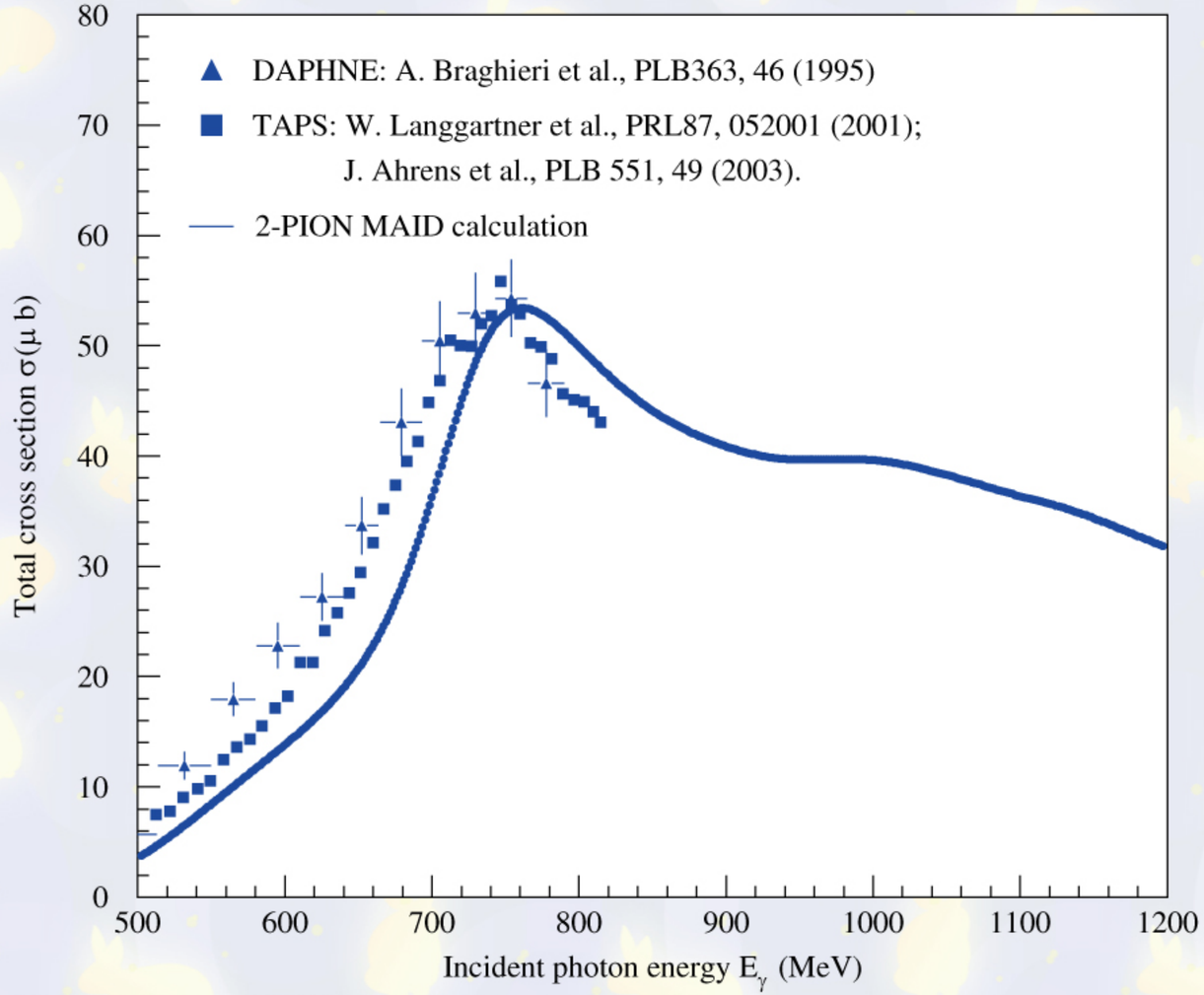

The published data

three papers from Mainz

below 800 MeV

2-PION MAID

not reproducing the data

N-Born and Δ-Born terms

8 resonances:

$P_{33}(1232)$, $P_{11}(1440)$, $D_{13}(1520)$, $S_{11}(1535)$,

$S_{31}(1620)$, $P_{31}(1720)$, $D_{15}(1675)$, $F_{15}(1680)$

Analysis for the $\gamma p \rightarrow \pi^0\pi^+ n$ reaction (H_2)

Total cross section as a function of E_γ

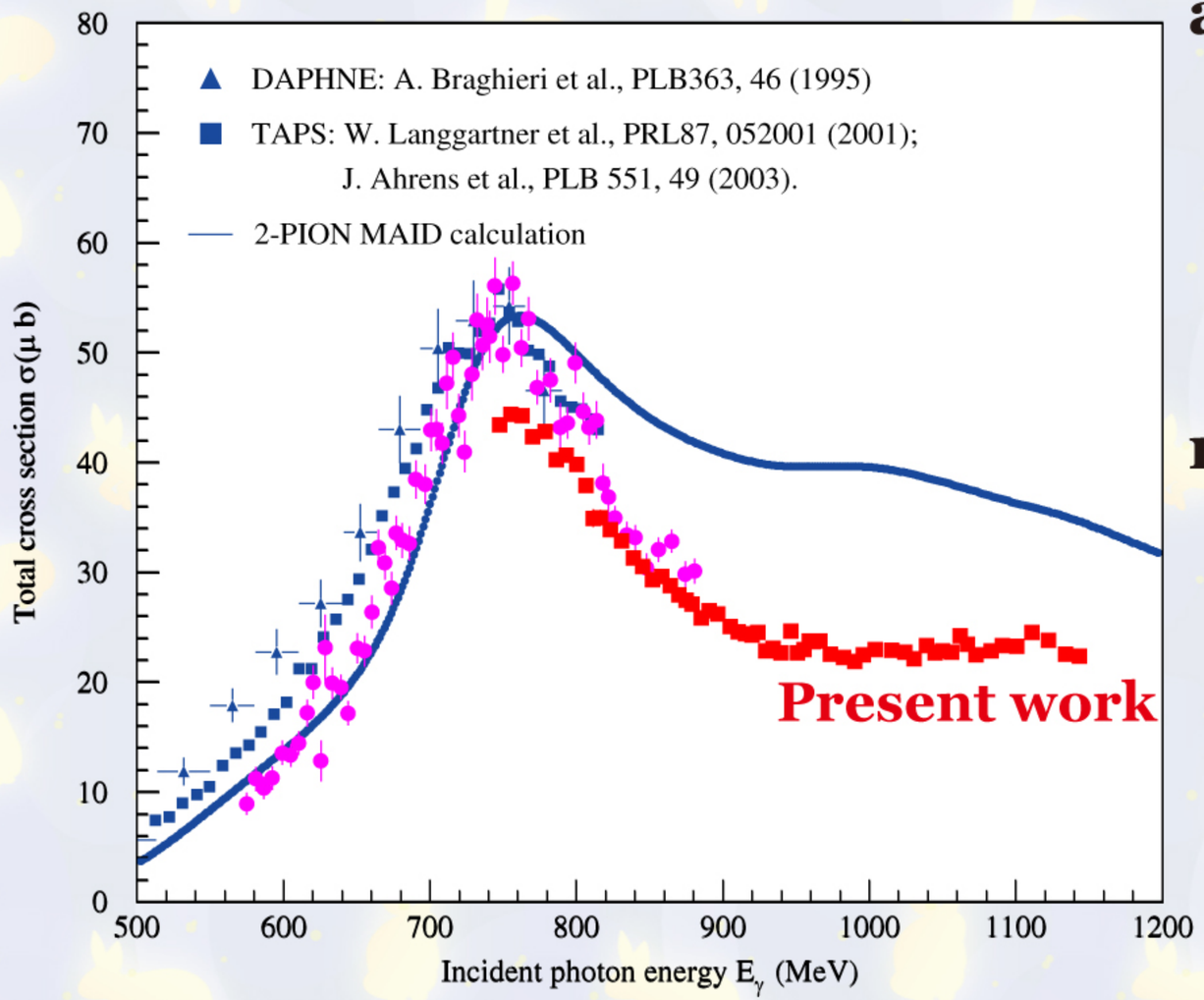

acceptance correction

- **event generation to reproduce the $M_{\pi^0\pi^+}$ vs $M_{\pi^0 n}$ correlation**
- **artificial efficiency correction for the neutron detection**

results

- **below 800 MeV**
  - **a little bit smaller cross section as compared with the previous data**
  - **consistent with the MAID calculation**
- **above 800 MeV**
  - **significantly different**

Analysis for the $\gamma p \to \pi^0\pi^+ n$ reaction (H_2)

Dalitz plot (W~1520 MeV)

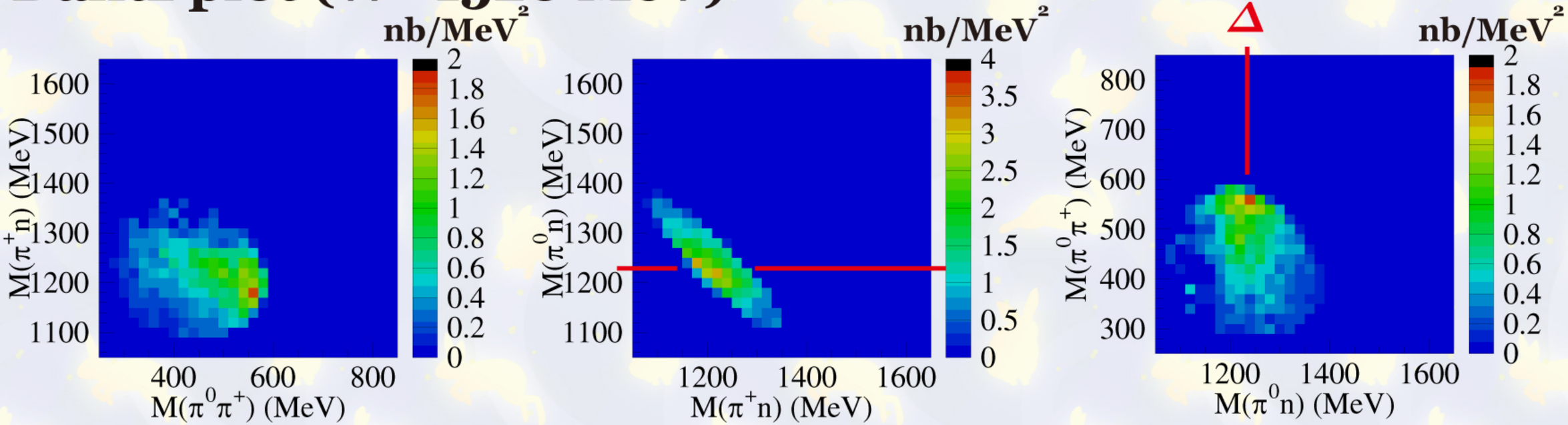

locus at $M(\pi^0 n)=M(\Delta)$:
Δ-Kroll-Ruderman term

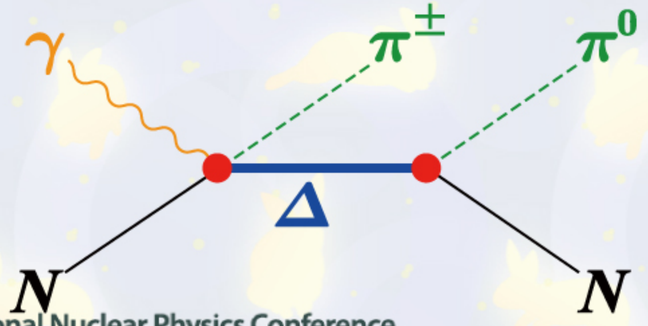

enhancement in the higher $M(\pi^0\pi^+)$:
ρ^+ production

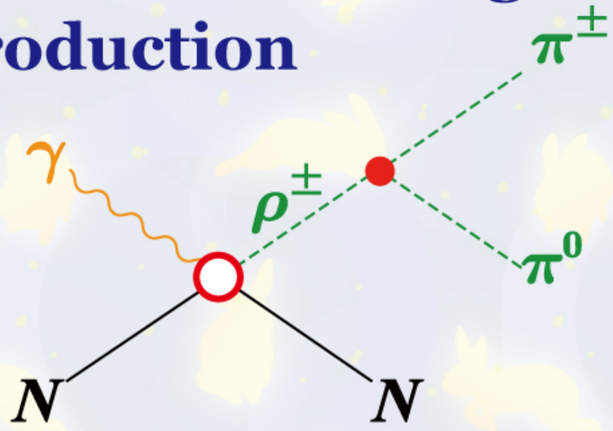

Analysis for the $\gamma p \to \pi^0\pi^+ n$ reaction (H_2)

Invariant mass distribution (W~1520 MeV)

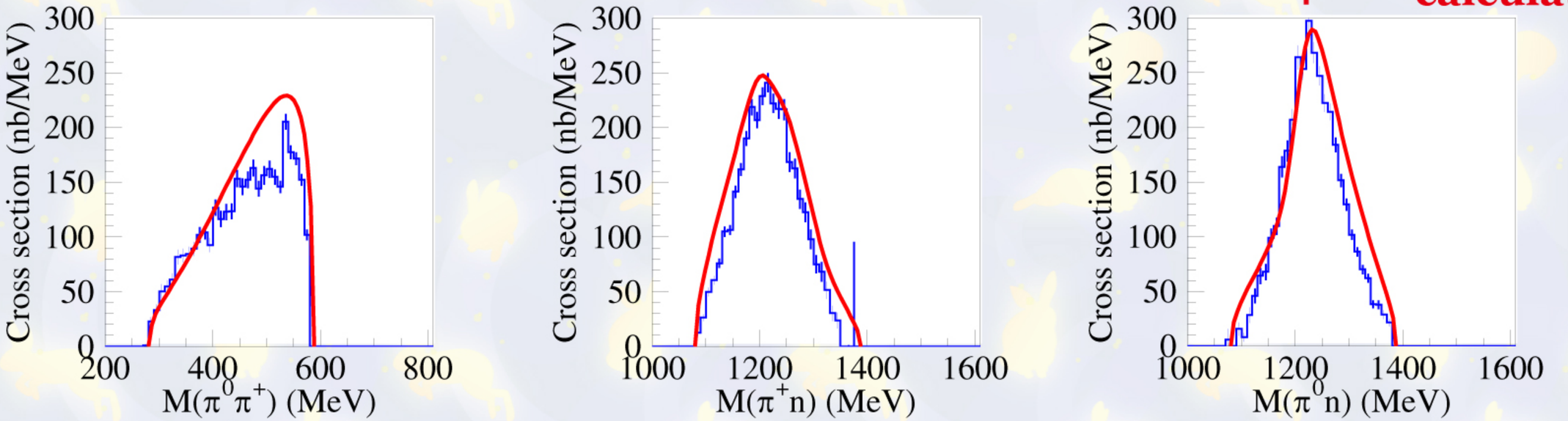

locus at $M(\pi^0 n)=M(\Delta)$: Δ-Kroll-Ruderman term

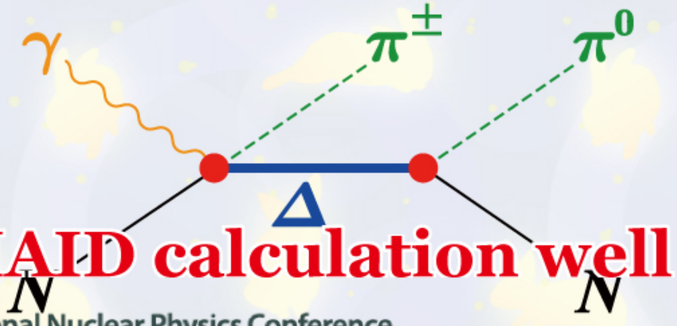

enhancement in the higher $M(\pi^0\pi^+)$: ρ^+ production

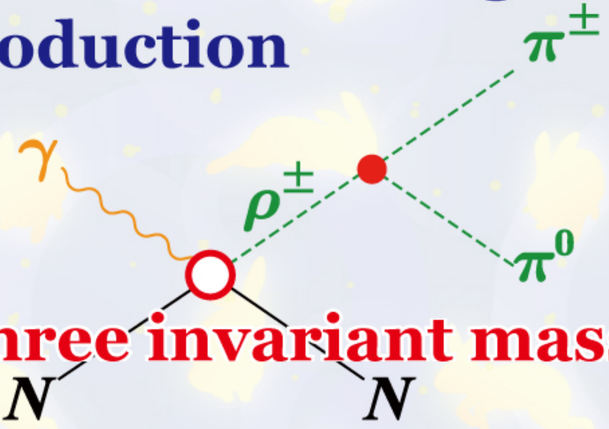

The MAID calculation well reproduces three invariant mass distributions

Analysis for the $\gamma p \to \pi^0\pi^+ n$ reaction (H_2)

Dalitz plot (W~1680 MeV)

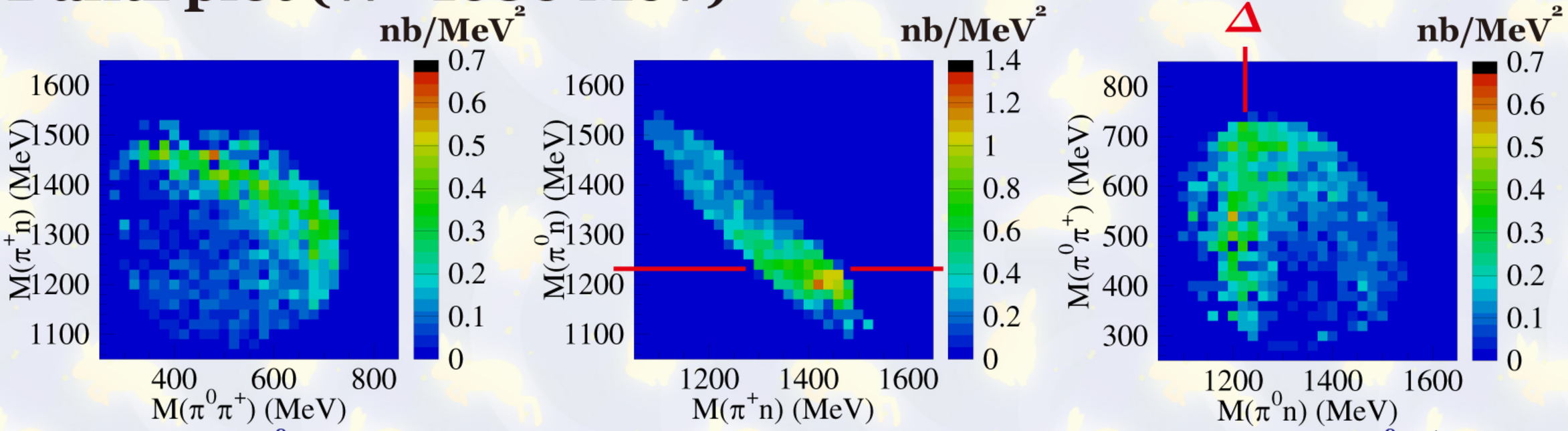

locus at $M(\pi^0 n)=M(\Delta)$:
Δ-Kroll-Ruderman term

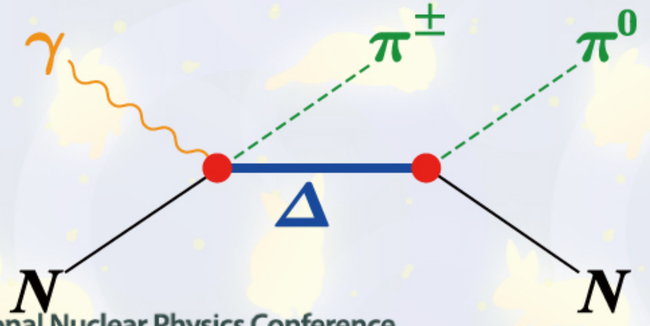

enhancement in the higher $M(\pi^0\pi^+)$:
ρ^+ production

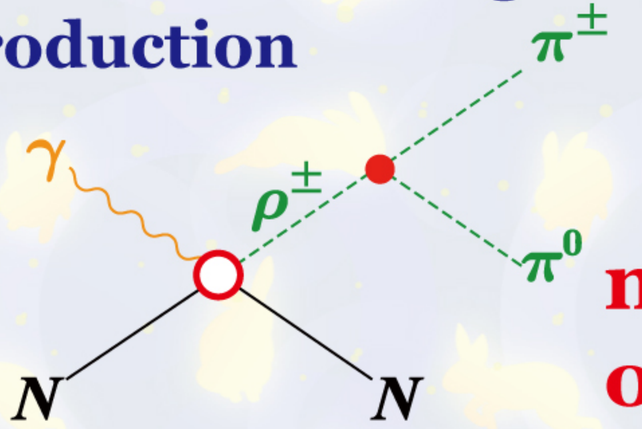

more clearly observed!

Analysis for the $\gamma p \to \pi^0\pi^+ n$ reaction (H_2)

Invariant mass distribution (W~1680 MeV)

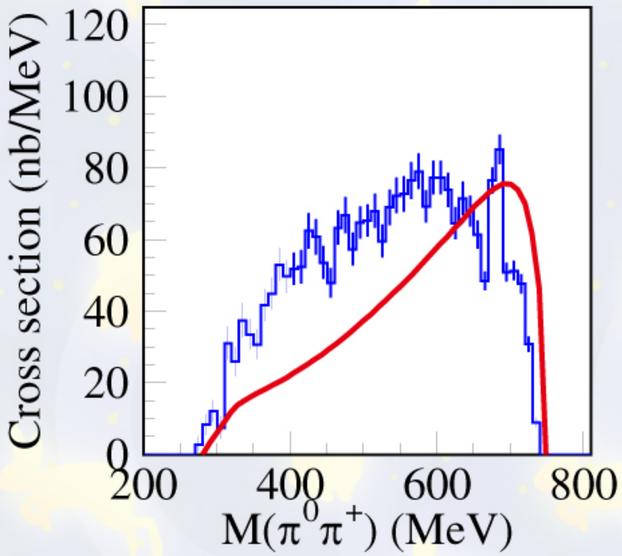

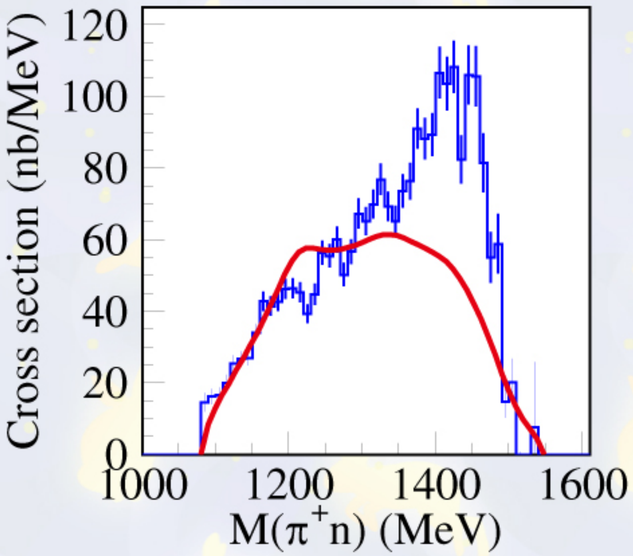

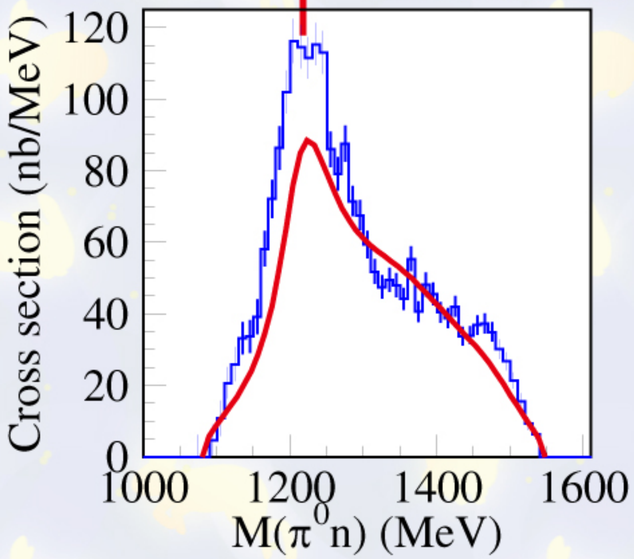

locus at $M(\pi^0 n)=M(\Delta)$:
Δ-Kroll-Ruderman term

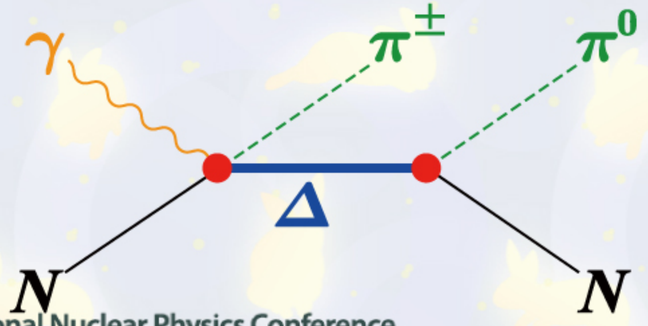

stronger

enhancement in the higher $M(\pi^0\pi^+)$:
ρ^+ production

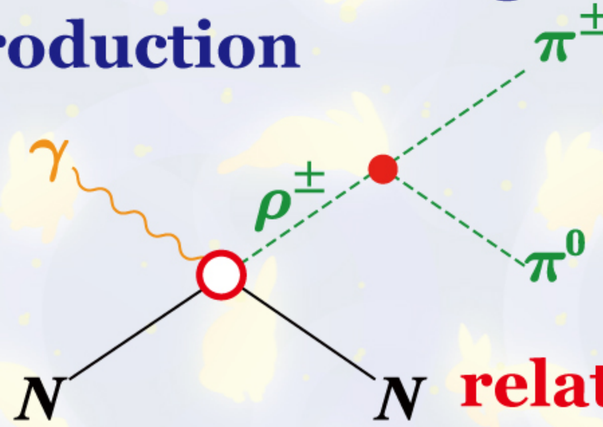

relatively weaker

Analysis for the $\gamma p \to \pi^0\pi^+ n$ reaction (H_2)

Angular distribution of ρ^+ mesons

$M(\pi^0\pi^+) \geqq 650$ MeV

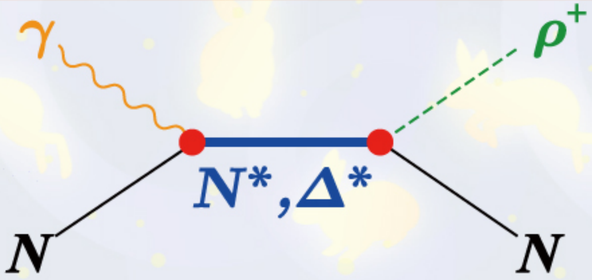

ρ^+ emission angle in the γp CM frame

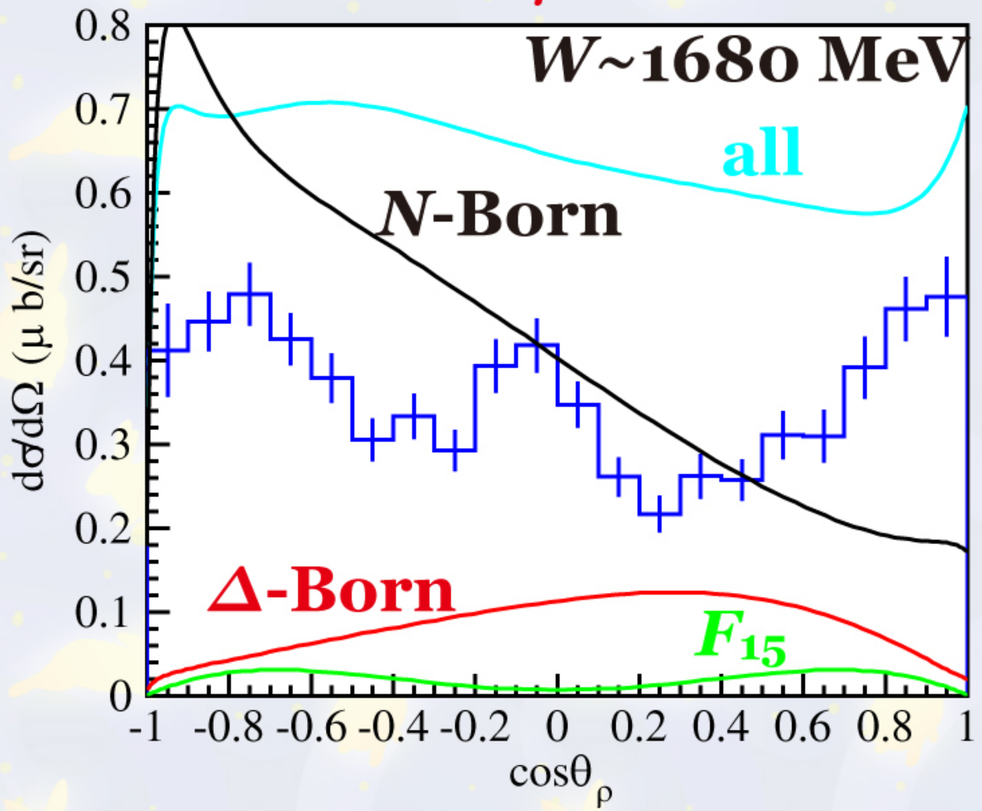

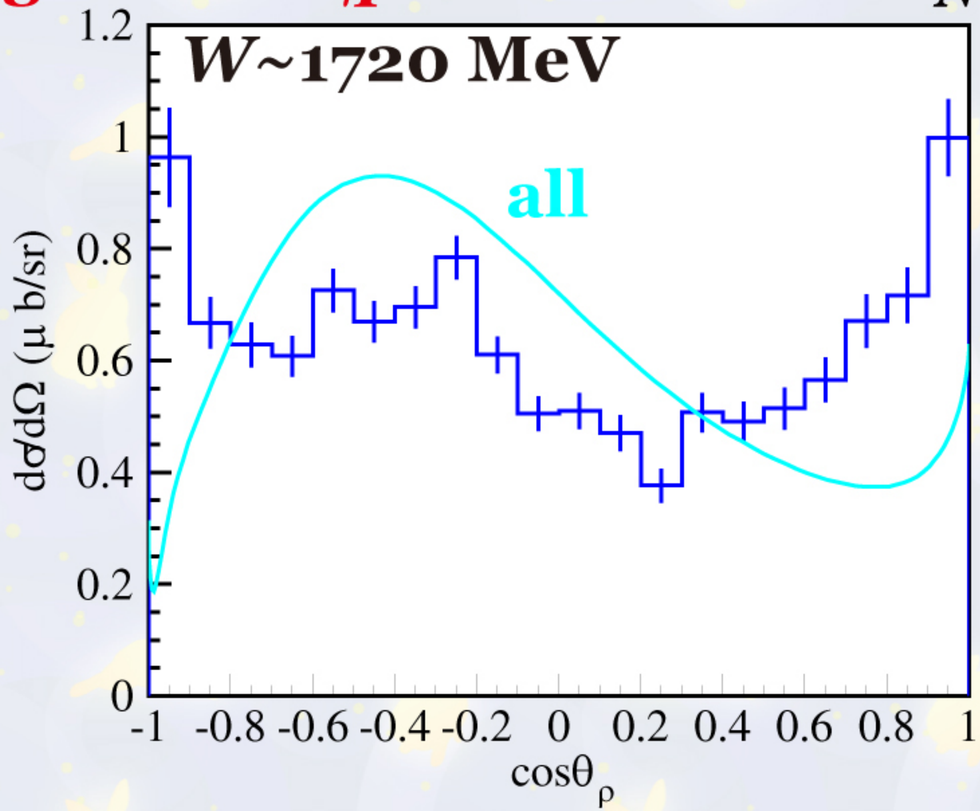

Destructive interference with F_{15} or higher J resonances

Analysis for the $\gamma p \to \pi^0 \pi^+ n$ and $\gamma n \to \pi^0 \pi^- p$ reaction (D_2)

Kinematical fit (4C)

constraints

- energy and momentum conservation (4)
- $\gamma\gamma$ invariant mass: π^0 (1)

variables

- incident photon energy (1)
- three-momenta for two γs (2×3)
- three-momentum of the nucleon (3)
- emission angle of the charged pion (2)
- Fermi motion of the target nucleon (3)

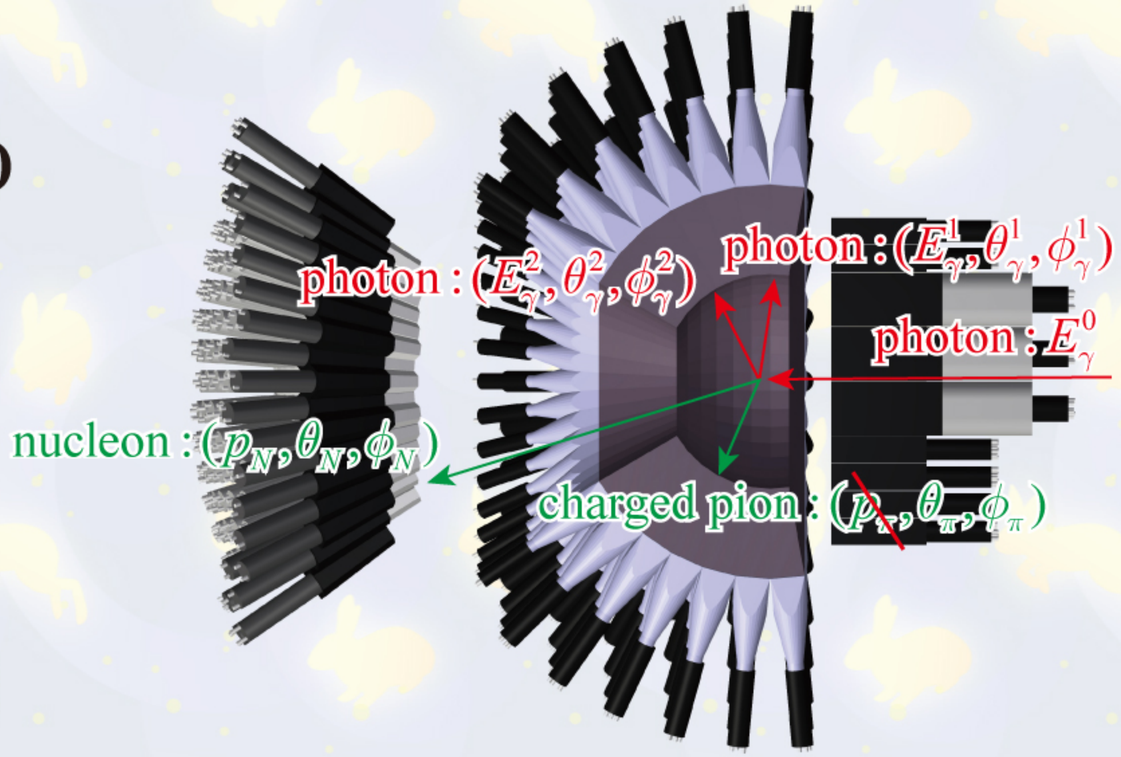

assuming the measured value is 40 MeV/c for each component

events in which χ^2 probability≧0.1 are selected

Analysis for the $\gamma p \to \pi^0\pi^+ n$ and $\gamma n \to \pi^0\pi^- p$ reaction (D_2)

Total cross section as a function of E_γ

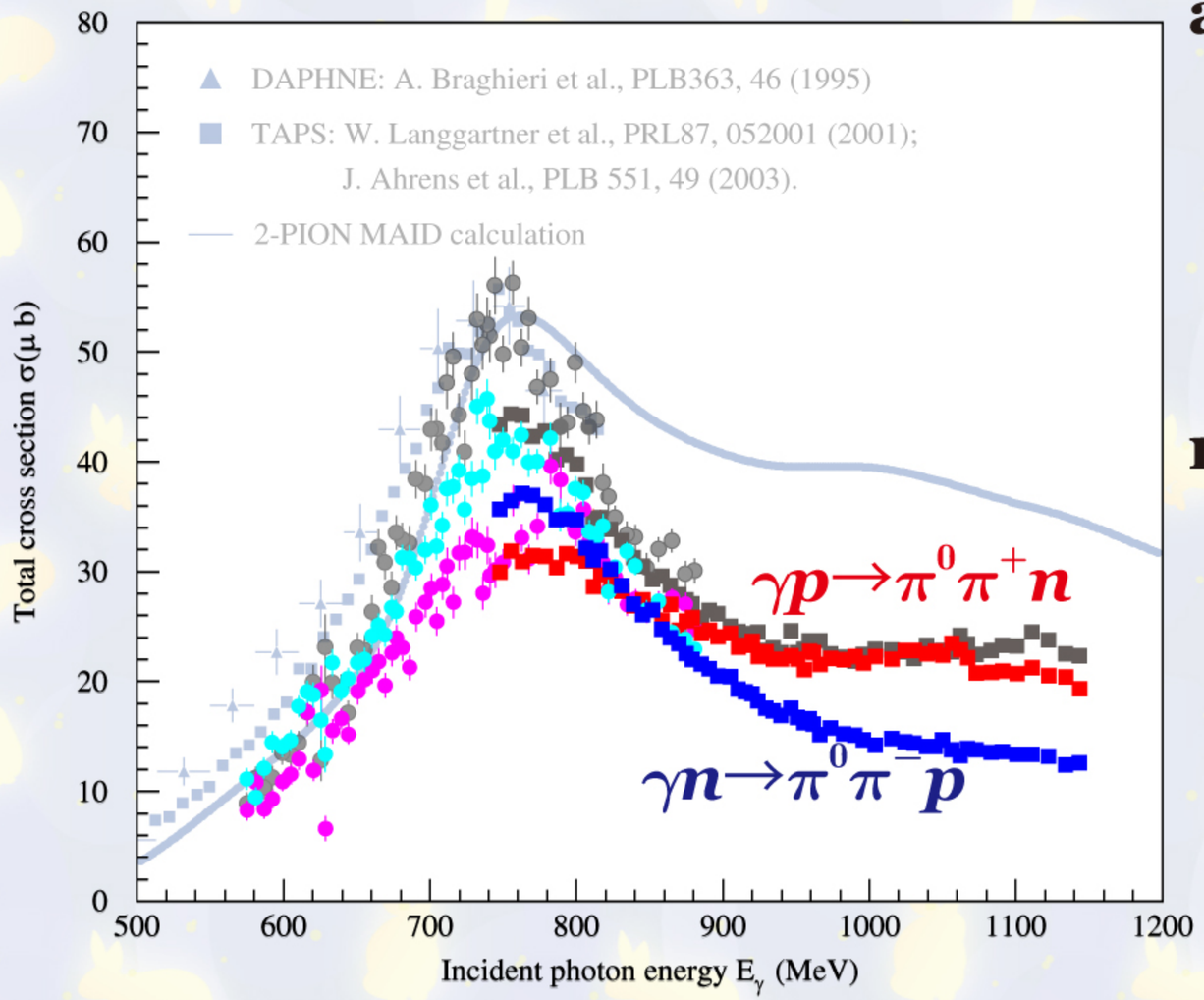

acceptance correction

- event generation to reproduce the $M_{\pi^0\pi^+}$ vs $M_{\pi^0 n}$ correlation
- artificial efficiency correction for the neutron detection

new results

- $\gamma n \to \pi^0\pi^- p$ is higher in the 2nd ersonance region
- $\gamma p \to \pi^0\pi^+ n$ is higher at high energies

Analysis for the $\gamma p \to \pi^0\pi^+ n$ and $\gamma n \to \pi^0\pi^- p$ reaction (D_2)

$\gamma p \to \pi^0\pi^+ n$

W~1680 MeV

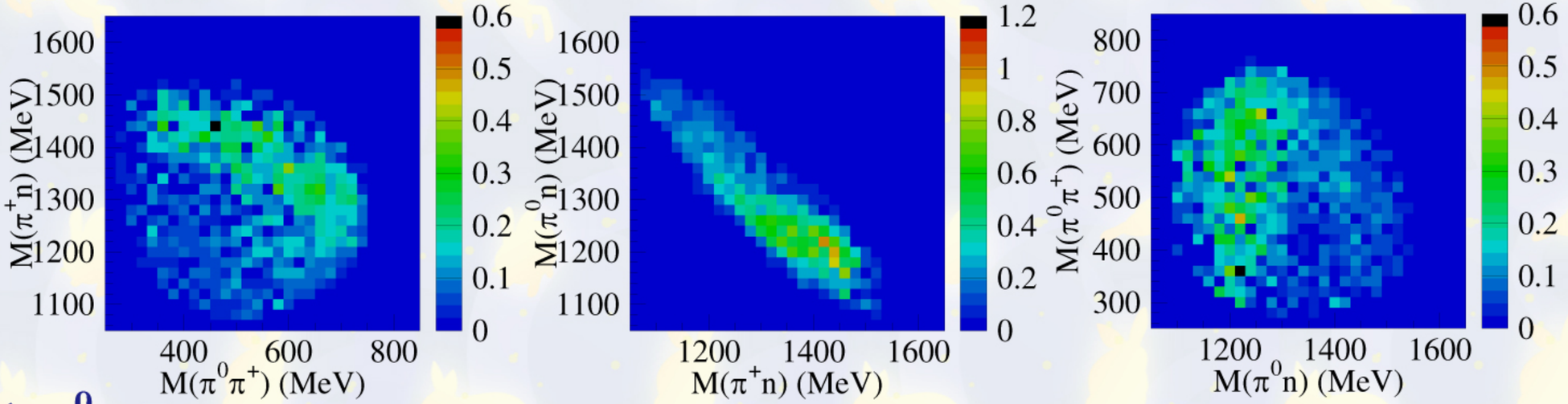

$\gamma n \to \pi^0\pi^- p$

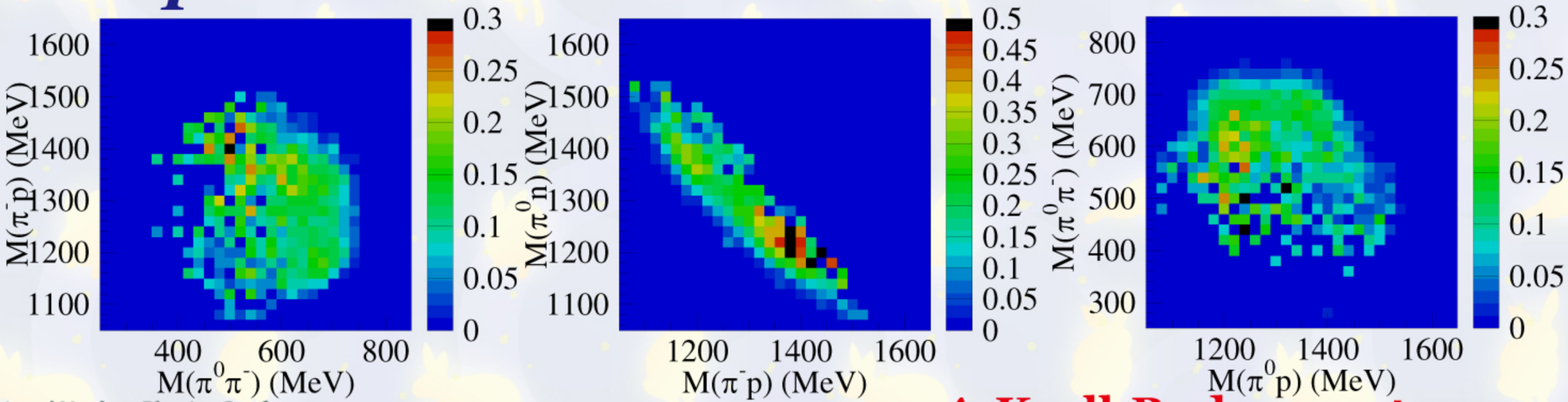

Δ-Kroll-Ruderman term: weaker

Analysis for the $\gamma p \to \pi^0\pi^+ n$ and $\gamma n \to \pi^0\pi^- p$ reaction (D_2)

Angular distribution of ρ^+ mesons

$M(\pi^0\pi^+) \geqq 650$ MeV

ρ^+ emission angle in the γp CM frame

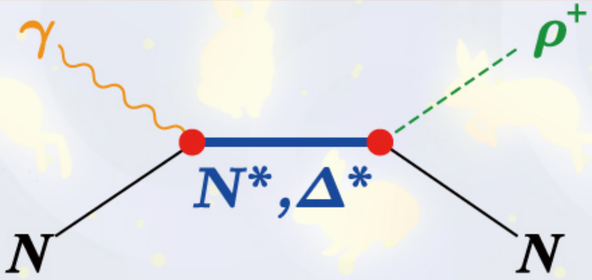

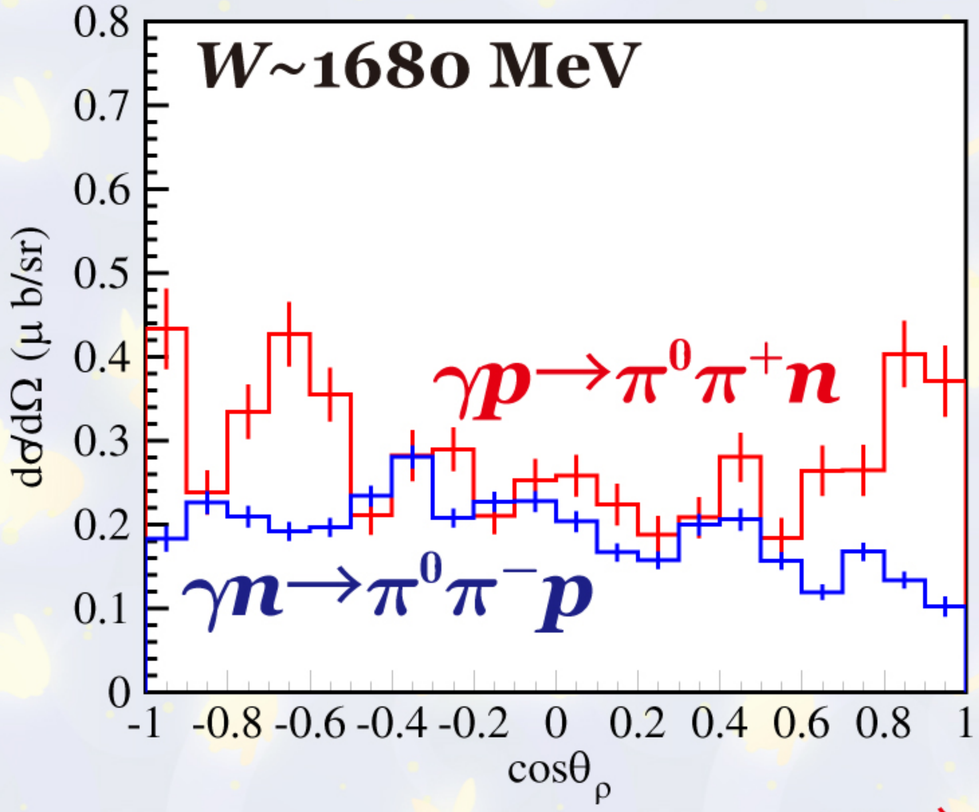

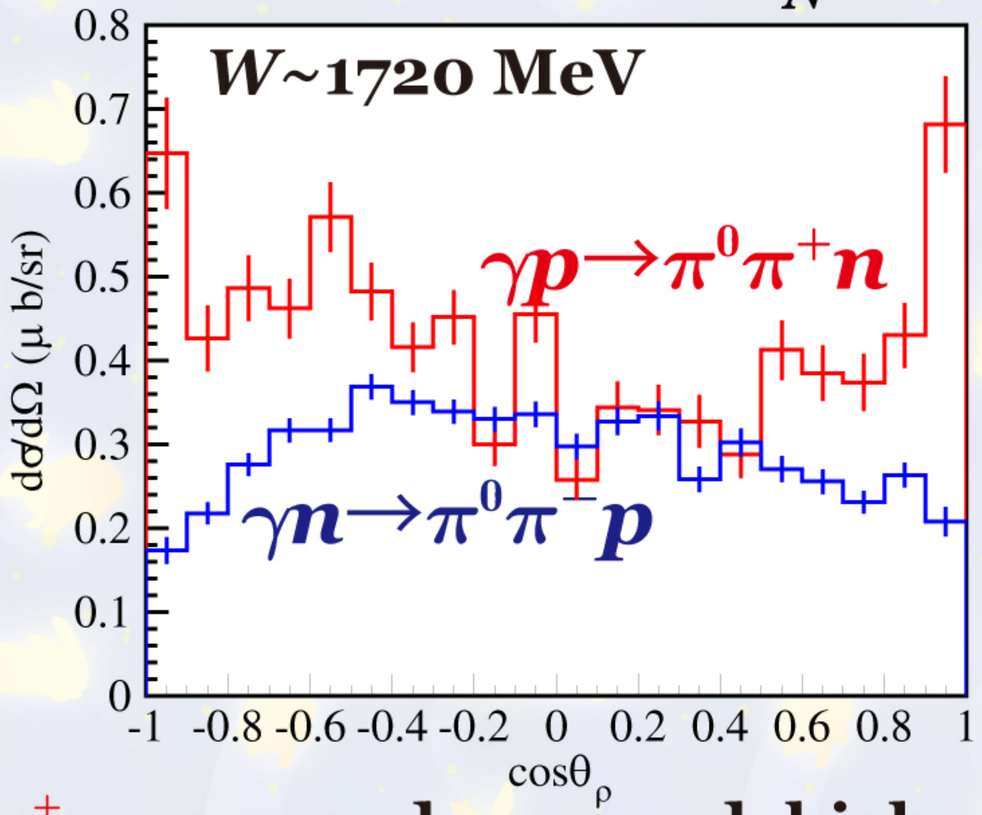

$\gamma p \to \pi^0\pi^+ n$: convex downward, higher J baryons?

$\gamma n \to \pi^0\pi^- p$: convex upward, J=3?

Summary

Meson photorpoduction experiments

were conducted using EM calorimeter FOREST at ELPH, Tohoku University.

$\gamma p \to \pi^0 \pi^+ n$ reaction (H_2)

expected to reveal the highly excited baryons

new data above 800 MeV

Δ-Kroll-Ruderman term and ρ^+ contributions

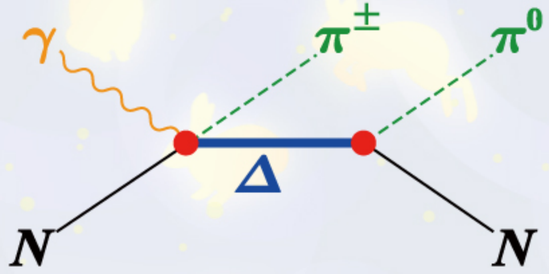

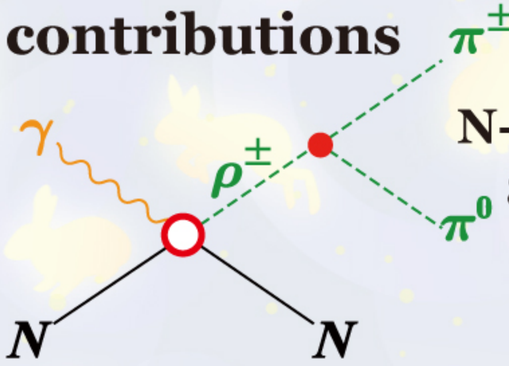

PWA analysis is desired

to reveal the baryon resonances.

N-Born and Δ-Born terms

8 resonances:

$P_{33}(1232)$, $P_{11}(1440)$, $D_{13}(1520)$, $S_{11}(1535)$,
$S_{31}(1620)$, $P_{31}(1720)$, $D_{15}(1675)$, $F_{15}(1680)$

2-PION MAID does not reproduce data at high energies

$\gamma p \to \pi^0 \pi^+ n$ and $\gamma n \to \pi^0 \pi^- p$ reaction (D_2)

Δ-Kroll-Ruderman term and ρ^+ contributions

weaker in $\gamma n \to \pi^0 \pi^- p$

Backup slides

Meson photoproduction for baryon spectroscopy

Mass spectum:
good agreement for differnt models below 1.6 GeV

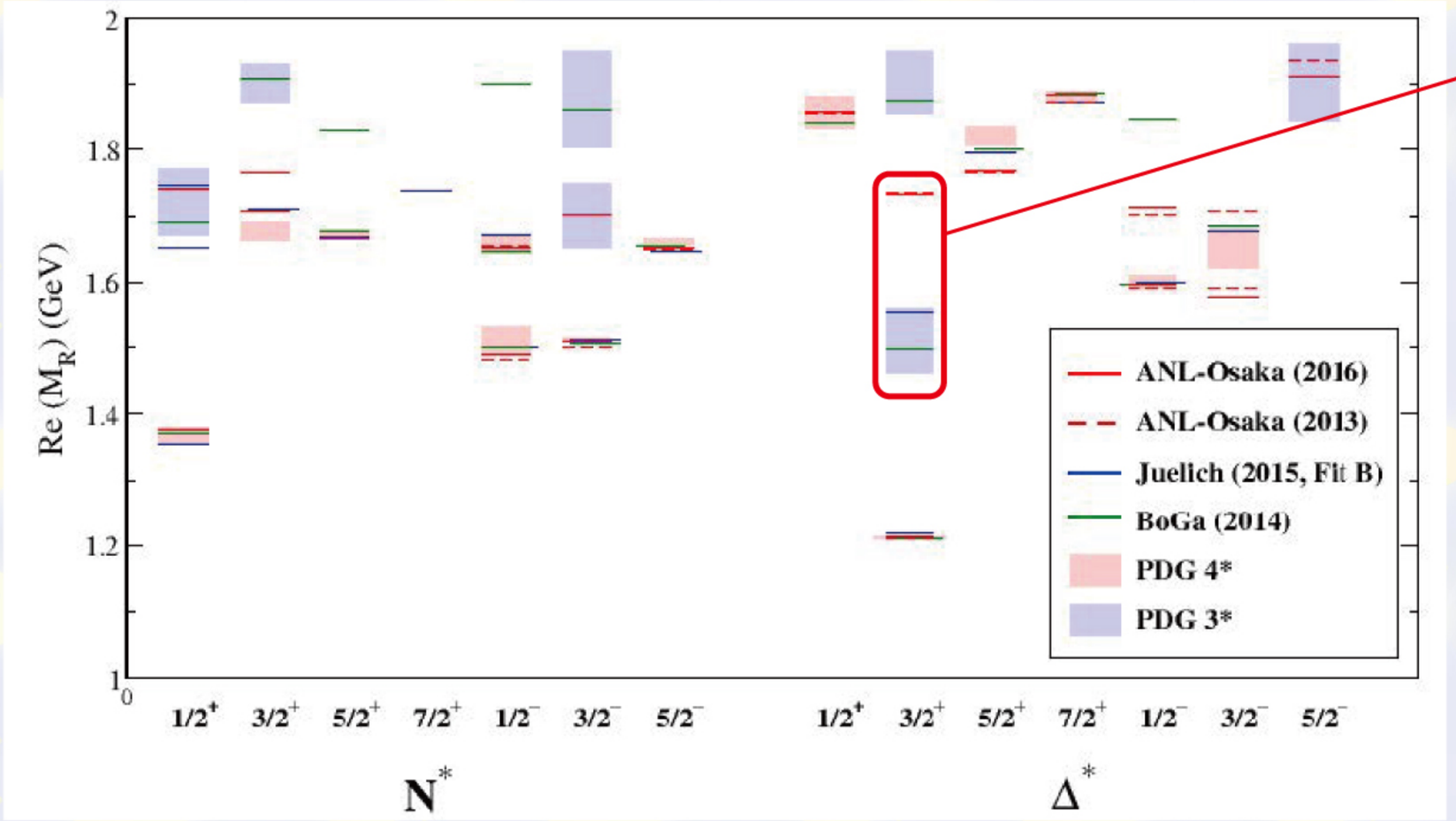

Roper-like Δ*
PDG 3*
different positions

H. Kamano, talk at MENU2016.

Analysis for the $\gamma p \rightarrow \pi^0 \pi^+ n$ reaction (H_2)

Detection efficiency

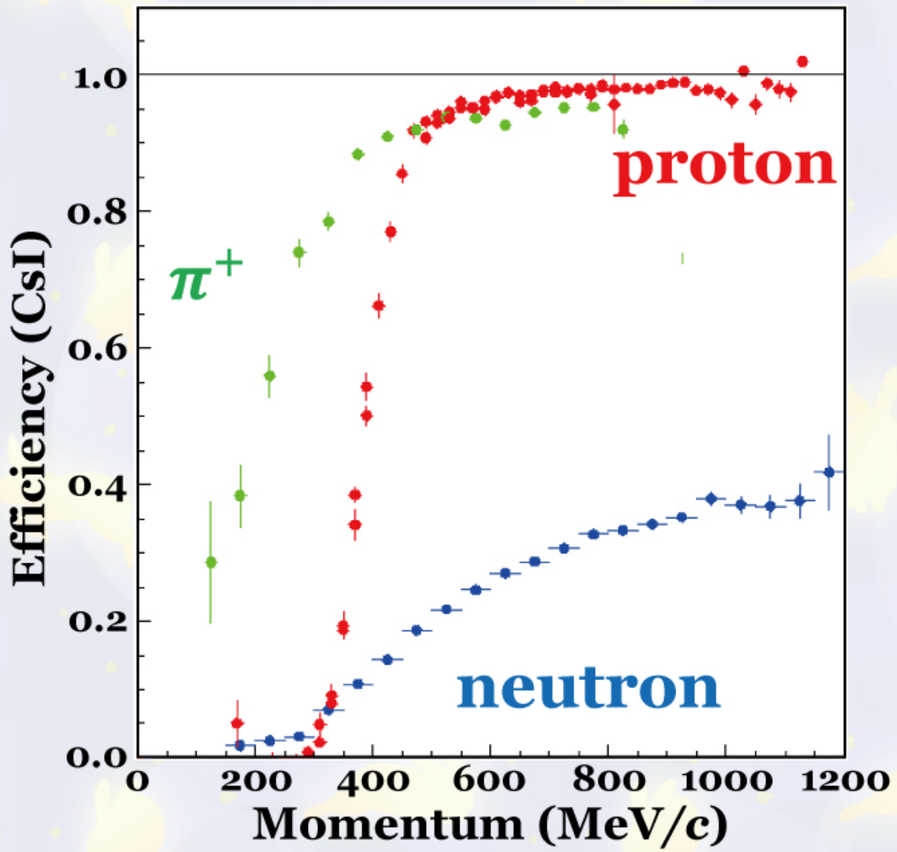

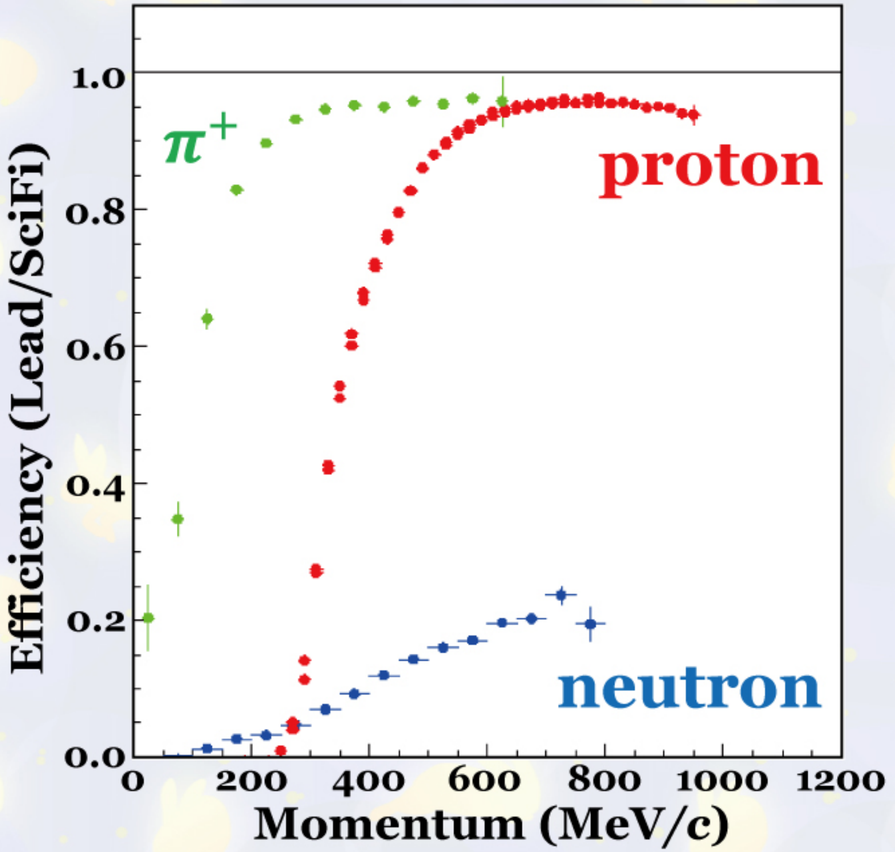

well-reproduced applying a discriminator threshold for charged particles

artificially corrected for the neutrons

Analysis for the $\gamma p \rightarrow \pi^0 \pi^+ n$ reaction (H_2)

Total cross section as a function of E_γ

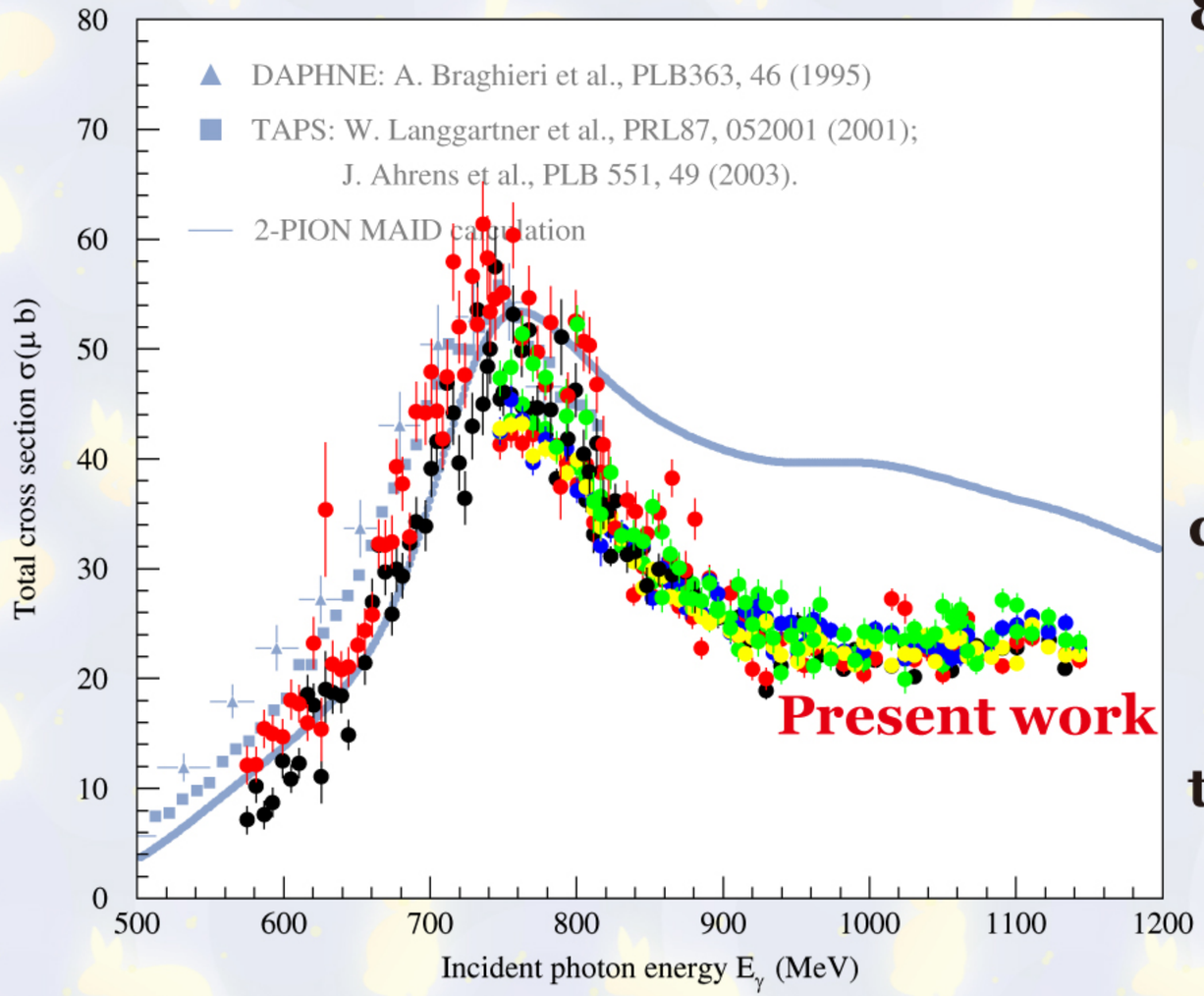

8 series of experiments

2 of them: 930 MeV mode

photon energy: 570~890 MeV

6 of them: 1200 MeV mode

photon energy: 740~1150 MeV

discriminator threshold

different for different series

the obtained cross section

consistent within 10% level